MDPI

Article

Modeling of a Three-Stage Cascaded Refrigeration System Based on Standard Refrigeration Compressors in Cryogenic Applications above 110 K

Zbigniew Rogala [1],* and Adrian Kwiatkowski [2]

1   Department of Cryogenics and Aerospace Engineering, Wroclaw University of Science and Technology, 50-370 Wrocław, Poland
2   CryoScience Poland, 55-040 Bielany Wrocławskie, Poland; adrian.kwiatkowski@cryosc.com
*   Correspondence: zbigniew.rogala@pwr.edu.pl

Abstract: More and more applications, such as natural gas liquefaction, LNG reliquefaction, whole body cryotherapy and cryopreservation, require cooling in the temperature range from 110 to 150 K. This can be achieved in systems using standard refrigeration compressors, which are reliable and cost-effective, but are subject to certain operating limits. This paper investigates the potential of a three-stage cascaded refrigeration system based on standard refrigeration compressors in this range of temperatures. The investigation takes into account the vital limitations of refrigeration compressors and aims to look for possible refrigerant configurations (taking into account PFCs, HFCs, HCs and HOs); performance limitations such as cooling power temperature and system COP; and the influences of system architecture (single-stage and two-stage compression). The paper investigates whether it is possible to design a three-stage cascaded refrigeration system using standard refrigeration compressors, and if so, at what cost? This investigation shows that the three-stage cascaded refrigeration system can reach the lowest temperature of 127 K with a COP of 0.179, which corresponds to a Carnot efficiency of 0.262. Moreover, systems based on natural refrigerants are found to be advantageous in terms of achieved temperatures compared to those that use synthetic refrigerants. Furthermore, only the application of R50 (methane) is shown to allow temperatures below 130 K to be achieved, and this is possible only in a two-stage compression cascade system. For most of the investigated configurations, the suction pressure must be below atmospheric pressure to thermally couple cascade stages.

Keywords: refrigeration compressors; cascaded refrigeration system; cryogenics above 110 K; cryotherapy

1. Introduction

The last few decades have been characterized by a significant increase in the importance of cryogenic applications above 110 K. This has mainly been due to the growing liquified natural gas (LNG) industry [1], which requires the solutions to either cool down and finally liquefy natural gas [2–9], or reliquify LNG boil-off [10,11], or upgrade biogas by cryogenic carbon dioxide removal [12]. Another emerging application and market is whole body cryotherapy [13], which requires between a few and tens of kilowatts of cooling power, cryoelectronics [14], cryopreservation [15], long-term storage [16] and cryomilling [17–20]. An overview of cryogenic applications above 110 K is presented in Figure 1.
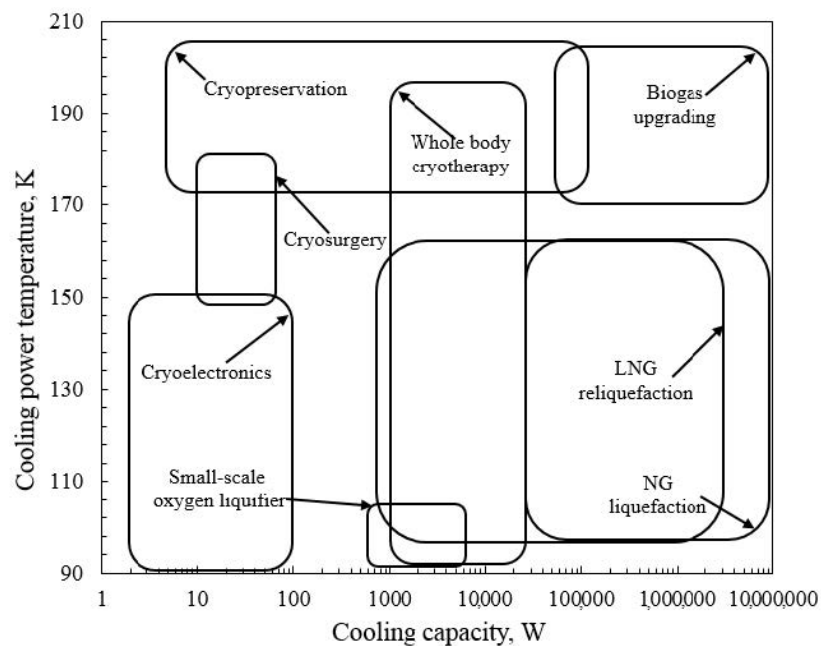
Figure 1. Overview of cryogenic applications above 110 K.

Cooling power within the temperature range of 110 to 150 K on an industrial scale is provided mainly by reverse Brayton cycles [8,10,21,22], Claude cycles [23], or Kapitza [10] and hydrocarbon-based cascade solutions [8,21]. These solutions are mainly used as refrigeration cycles of LNG boil-off gas reliquefaction systems. In addition to industrial-scale systems, the increase in demand for cooling power at temperatures above 110 K requires the development of new solutions dedicated to smaller capacities, such as cascade cryorefrigerators [4–6,24,25], mixed-refrigerant Joule–Thomson cryocoolers [26–30], combined cascade solutions [31–33] and modified Joule–Thomson cryocoolers [26,34]. Some of these solutions can be based on standard mass-produced refrigeration compressors [27–29]. Standard refrigeration compressors are cost-effective and reliable solutions, but on the other hand, they are subject to strict limitations in terms of operating pressures and temperatures. Due to these limitations, some of the proposed systems based on standard refrigeration compressors cannot be built at very high discharge pressure [5,6,9], very low suction temperatures [11], or very high discharge temperatures [31]. This article aims to assess the potential of three-stage cascaded cryorefrigerators based on standard refrigeration compressors in cryogenic applications above 110 K. The investigation includes an analysis of the available refrigerant configurations, modeling of the system under the operating limitations of the refrigeration compressors and a study of the influences of the system architecture. The study provides vital information on the feasibility and performance limits of three-stage cascaded cryorefrigerators. According to the authors' knowledge, similar work has not been published yet.

2. Materials and Methods

The analysis carried out aimed to assess the applicability of different refrigerants characterized by $ODP = 0$ in the three-stage cascaded cryofrigerator model. To be classified as applicable, the refrigerant must enable thermal coupling with heat sources: within specified ranges of suction and discharge pressures, with sufficiently low discharge temperature. According to European regulations on fluorinated greenhouse gases and the regulation [35] from 1 January 2020, the use of fluorinated greenhouse gases, with a GWP of 2500, is prohibited, with the exception of military use and applications designed to cool products to temperatures below $-50\ ^\circ\text{C}$. Therefore, in the application considered, the use of refrigerants with global warming potentials (GWPs) greater than 2500 is exceptionally allowed. A similar study was carried out by [31]. Furthermore, due to the maximum allowable

pressure of refrigeration compressors of 30 bar [36–40] and the limitation of the suction pressure to at least 0.2 bar [41,42], the refrigerant should allow its stage to be coupled with the neighboring one. Several single component refrigerants were taken into account. Some of the initially included refrigerants, such as R161, R218, R22, R32, R41, and R143a, were found not to be applicable due to strict operational limits; it was not possible to thermally couple them to other cascade stages. The condensation or evaporation temperatures do not match the temperatures of the neighboring stages, and a further increase in discharge pressure or decrease in suction pressure was not possible due to the operational limitations of the compressors. The remaining refrigerants are briefly described in Table 1 and their saturation curves are presented in Figure 2. The analysis considered non-flammable (A1), flammable (A2, A2l and A3) and zero-ODP refrigerants. The saturation curves were drawn at 0.5 bar. One can see that only flammable R50 allows temperatures below 125 K. On the other hand, R50 is characterized by a critical temperature of 190.6 K, which means that to apply this natural refrigerant as a third stage working fluid, it is required to reach the temperature of 185.6 K by means of only two stages. Moreover, substantial differences in the heat of evaporation between natural refrigerants (HCs and HOs) and synthetic refrigerants (CFCs, HFCs and PFCs) can be seen. This affects the required mass and volumetric flows of the refrigerant.

Table 1. Thermodynamic data of the refrigerants considered [43].

Fluid	Type	ODP	GWP	FC [1]	T_{sat} (1 bar)	T_{sat} (0.2 bar)	T_{sat} (30 bar)	T_{cr}	p_{cr}	ΔH_{ev} (1 bar)	T_{TP}
-	-	-	-	-	K	K	K	K	bar	kJkg^{-1}	K
R1270	HO	0	1.8	A3	225.2	195.3	341.8	364.2	45.6	439	87.953
R290	HC	0	3.3	A3	230.7	199.8	350.9	369.9	42.5	426	85.525
R125	HFC	0	3170	A1	224.8	196.9	330.6	339.2	36.2	164	172.52
R116	PFC	0	12,200	A1	194.8	173.6	292.4	293	30.5	117	173.1
R1150	HO	0	3.7	A3	169.2	146.1	260	282.4	50.4	483	103.989
R170	HC	0	5.5	A3	184.3	159.1	282.9	305.3	48.7	490	90.368
R23	HFC	0	12,400	A1	190.9	167.1	280.1	299.3	48.3	240	118.02
R50	HC	0	28	A3	111.5	95.1	177.3	190.6	46	511	90.694
R14	PFC	0	7390	A1	144.9	125.5	220	227.5	37.5	135	120

1—Flammability class, A1: nonflammable, A2L: lower flammable, A3: highly flammable.
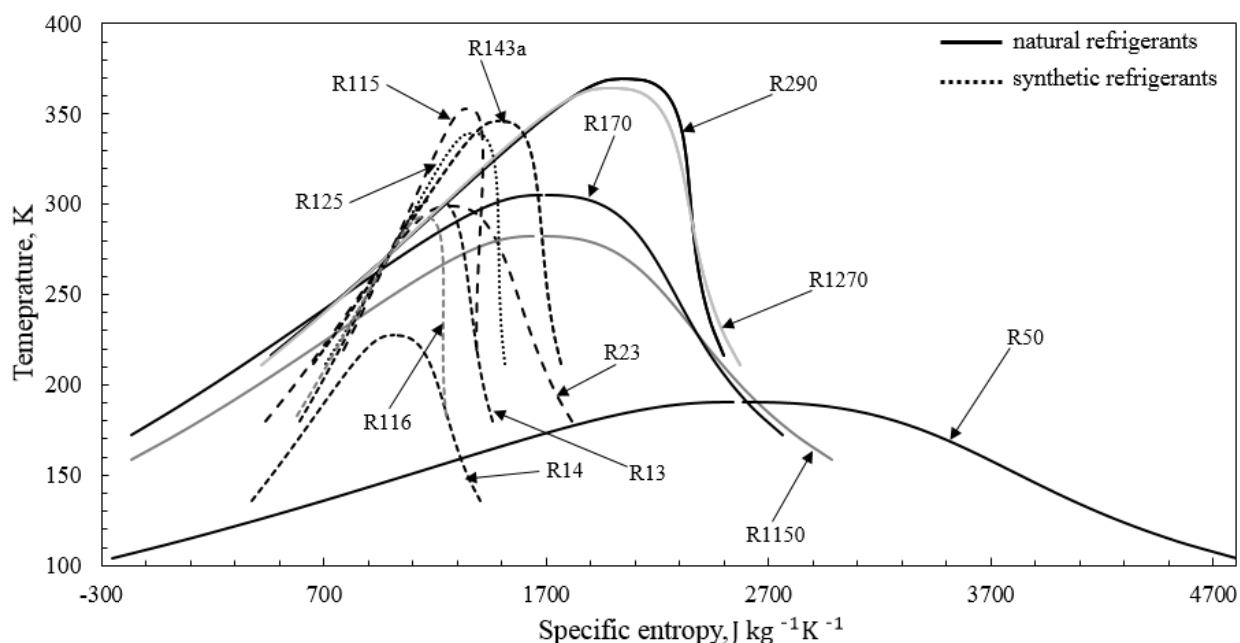

Figure 2. Saturation curves of the refrigerants considered [43].

The analysis was carried out for two different configurations of the three-stage cascaded refrigeration systems, which are presented in Figures 3 and 4. The first system considered, presented in Figure 3, applies only single-stage compression at each stage. The second configuration, presented in Figure 4, is more complex, having compression in two stages, in the second and third stages. These two configurations were chosen to highlight the performance improvement achieved at the expense of a more complex system architecture. Two-stage compression was not considered in the first stage, as this stage is actually a typical refrigeration cycle which is unlikely to operate with two-stage compression. In addition to the cascade systems schemes analyzed, Figures 2 and 3 also contain Ts diagrams for each stage with the given characteristic points of the systems. To model the performance of the whole system, all the thermodynamic states at each stage have to be determined. This was performed using CoolProp [44], which is an open thermodynamic database packaged with Python and Excel. The thermodynamic state was determined for the known pair out of five considered thermodynamic parameters: temperature, pressure, enthalpy, entropy, and quality. The design procedure of each stage is similar; therefore, it is presented using the example of the second stage with two-stage compression. Initially, the assumption of the stage evaporation temperature $T_{evap,2}$ and the stage mass flow rate $\dot{m}_2$ is made. The modeling takes into account the assumed pressure losses of the heat exchangers, which are consistent with [3] and are given in Table 2. The isentropic efficiency of the compressors is not constant and depends on several operational factors, such as the compressed fluid's pressure ratio, as shown in Figure 5. It typically ranges from 60 to 75% [36,45,46]. There is no comprehensive work describing the method for obtaining the actual efficiency of the compressor, and therefore it is very common to assume this value as constant even in very extensive analyses that include different sets of fluids and operating conditions [26,47–50]. Isentropic efficiencies generally range from 60% [50] to 80% [26,48,51], but an isentropic efficiency of 100% can also be found [49,52,53]. Moreover, manufacturers generally specify the minimum suction gas temperature [36,38].
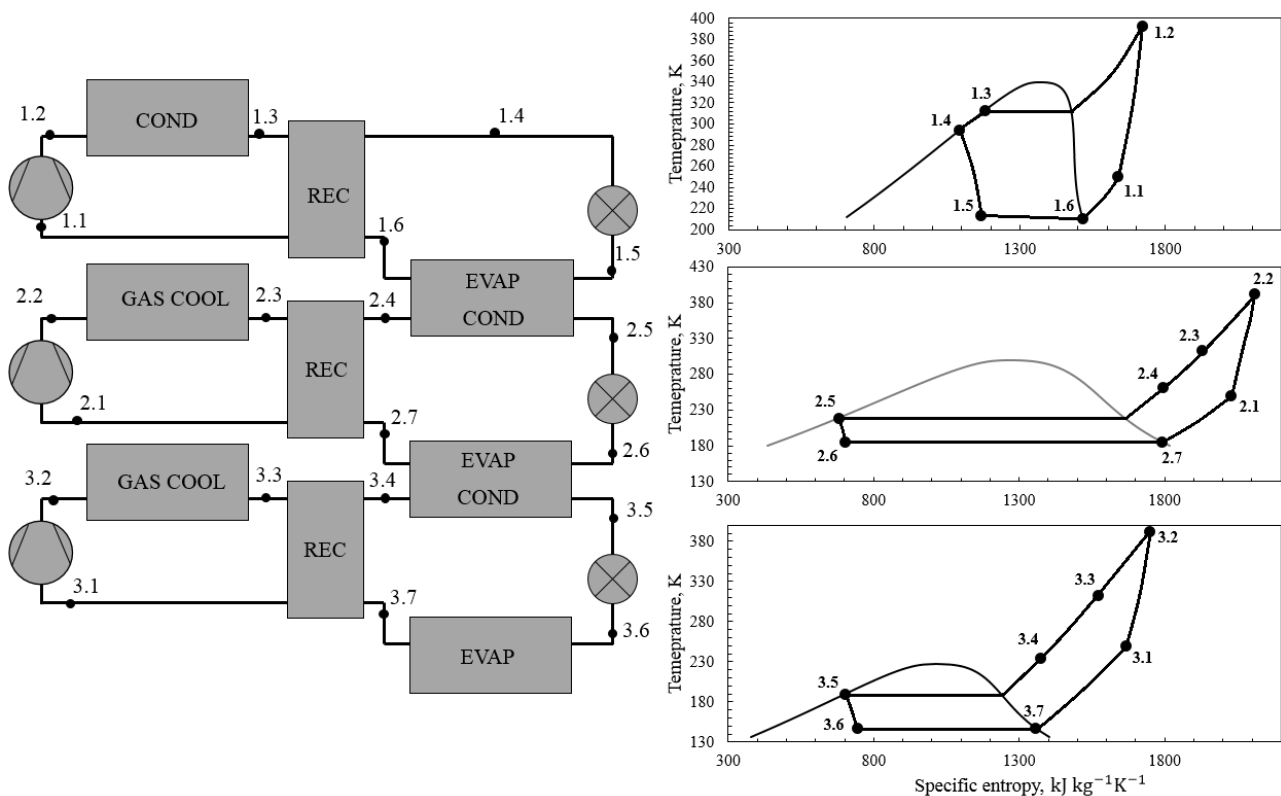

Figure 3. The scheme of the three-stage cascaded refrigeration system with single-stage compression.
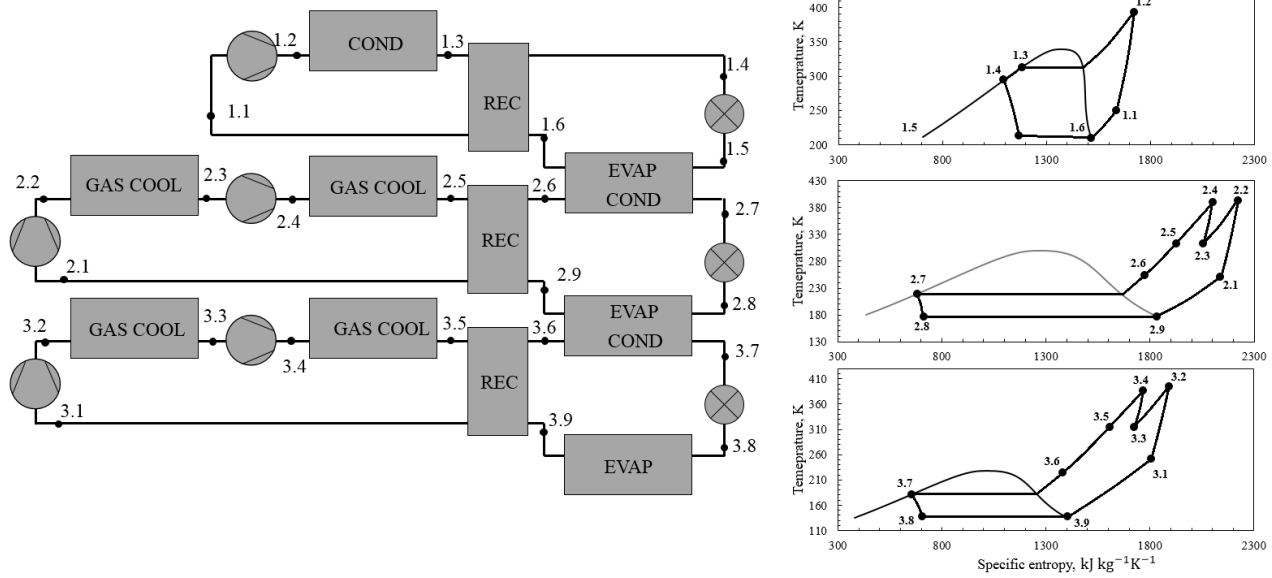
Figure 4. The scheme of a three-stage cascaded refrigeration system with two-stage compression.
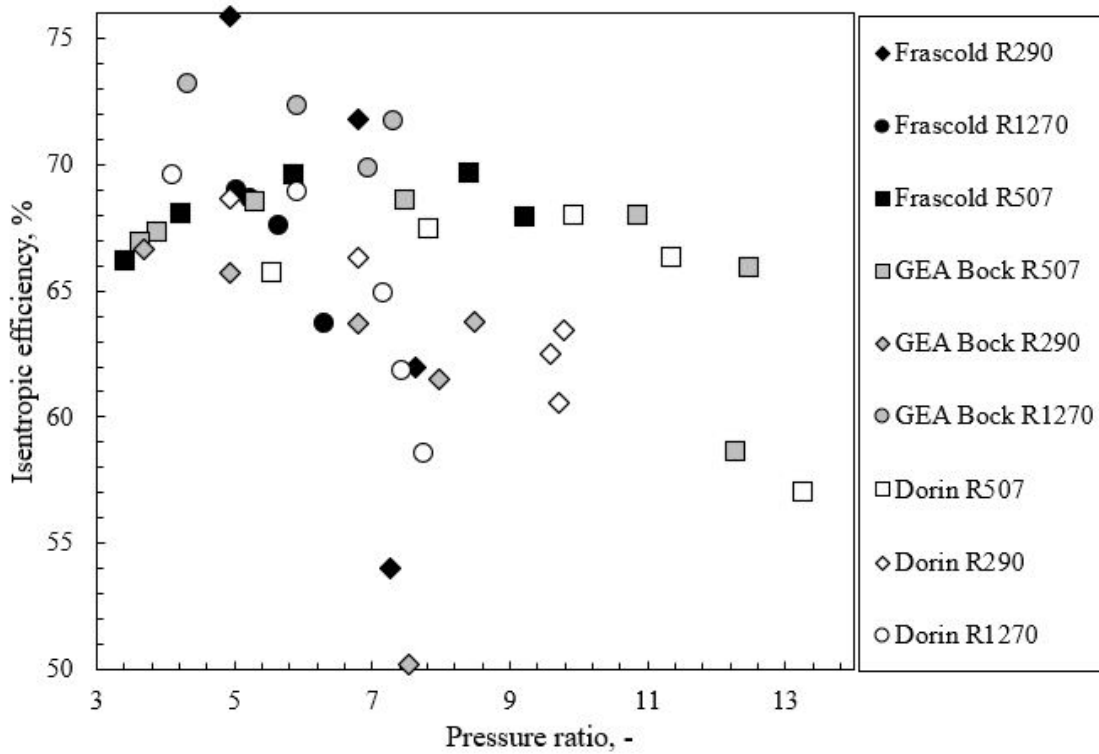

Figure 5. Isentropic efficiency with respect to the pressure ratio of semi-hermetic refrigeration compressors estimated using the dedicated selection software provided by the manufacturers [36,45,46].

The condensing pressure is determined on the basis of the higher-stage evaporation temperature.

$$p_{2.7} = f(T_{2.7} = T_{1.5} + \Delta T_{e-c}, Q_{2.7} = 0) \tag{1}$$

This allows us to determine all the pressures on the high-pressure side:

$$p_{2.6} = p_{2.7} + \Delta p_{cond} \tag{2}$$

$$p_{2.5} = p_{2.6} + \Delta p_{rec,HP} \tag{3}$$

$$p_{2.4} = p_{2.5} + \Delta p_{gascool} \tag{4}$$

The pressures on the low-pressure side are governed by the evaporation temperature $T_{1.5}$:

$$p_{2.8} = f(T_{2.8}, Q = 1) \tag{5}$$

$$p_{2.9} = p_{2.8} - \Delta p_{evap} \tag{6}$$

$$p_{2.1} = p_{2.9} - \Delta p_{rec,LP} \tag{7}$$

Pressures between compression stages $p_{2.2}$ and $p_{2.3}$ are determined on the basis of the pressure ratio $\pi_{comp,2.1}$:

$$p_{2.2} = \frac{p_{2.4}}{\pi_{comp,2.1}} \tag{8}$$

$$p_{2.3} = p_{2.2} - \Delta p_{gascool} \tag{9}$$

Temperatures $T_{2.1}$, $T_{2.3}$, and $T_{2.5}$ are determined based on modeling assumptions.

$$T_{2.1} = T_M - \Delta T_{rec} \tag{10}$$

$$T_{2.3} = T_{2.5} = T_M \tag{11}$$

Thermodynamic states at the compressor discharges are determined using isentropic compression as a reference:

$$h_{2.2s} = f(p_{2.2}, s_{2.2} = s_{2.1}) \tag{12}$$

$$h_{2.4s} = f(p_{2.4}, s_{2.4} = s_{2.3}) \tag{13}$$

$$h_{2.2} = h_{2.1} + \frac{h_{2.2s} - h_{2.1}}{\eta_{comp,s}} \tag{14}$$

$$h_{2.4} = h_{2.3} + \frac{h_{2.4s} - h_{2.3}}{\eta_{comp,s}} \tag{15}$$

The thermodynamic state 2.6 is evaluated using the recuperator heat balance:

$$h_{2.6} = h_{2.5} - (h_{2.1} - h_{2.9}) \tag{16}$$

The specific enthalpy of 2.8 is determined as follows:

$$h_{2.8} = h_{2.7} \tag{17}$$

The modeling parameters for Equations (1)–(17) are given in Table 2

Table 2. The modeling parameters.

Name	Symbol	Unit	Value	Reference
Heat rejection temperature	T_M	K	313	-
Compressor isentropic efficiency	$\eta_{comp,s}$	%	70	[37]
Stage temperature difference	ΔT_{e-c}	K	5	-
Pressure drop in condensers	Δp_{cond}	bar	0.1	[3]
Pressure drop in evaporators	Δp_{evap}	bar	0.1	[3]
Pressure drop in gas coolers	$\Delta p_{gascool}$	bar	0.2	[3]
Pressure drop in recuperator at high-pressure side	$\Delta p_{rec,HP}$	bar	0.1	[3]
Pressure drop in recuperator at low-pressure side	$\Delta p_{rec,LP}$	bar	0.1	[3]

The results are then iterated, according to the procedure presented, in order to meet the requirements of saturated liquid at point 2.7 and to get close to the operating limits. Therefore, the results can be interpreted as limiting the performance of the system. The method of determining the thermodynamic state of the characteristic points of the system is summarized in Table 3.

Table 3. The modeling of thermodynamic state in system characteristic points.

Point	T, K	p, bar	h, J kg^{-1}	s, J kg^{-1}K^{-1}	Q, -
2.1	$T_M - \Delta T_{rec}$	$p_{2.9} - \Delta p_{gascool}$			
2.2 s		$p_{2.4}/\pi_{comp,2.1}$		$s_{2.1}$	
2.2		$p_{2.2s}$	$h_{2.1} + \frac{h_{2.2s-h_{2.1}}}{\eta_{comp,s}}$		
2.3	T_M	$p_{2.2} - \Delta p_{gascool}$			
2.4 s		$p_{2.5} + \Delta p_{gascool}$		$s_{2.3}$	
2.4		$p_{2.4s}$	$h_{2.3} + \frac{h_{2.4s-h_{2.3}}}{\eta_{comp,s}}$		
2.5	T_M	$p_{2.6} + \Delta p_{rec,HP}$			
2.6		$p_{2.7} + \Delta p_{cond}$	$h_{2.5} - (h_{2.1} - h_{2.3})$		
2.7	$T_{ev1} + \Delta T_{e-c}$				$Q_{2.7} = 0$
2.8	T_{ev2}		$h_{2.7}$		
2.9		$p_{2.8} - \Delta p_{evap}$			$Q_{2.7} = 1$

The aim of this paper is to point out the operational limits of three-stage cascaded refrigeration systems consisting of typical refrigeration equipment: compressors, heat exchangers, expansion valves, etc. Therefore, the operation of each stage was designed to reach the operational limits of the most crucial components of this kind of system—the compressors. Other elements do not introduce significant operational limitations that should be taken into account. The operation limitations of the refrigeration compressors are based on the manufacturer's specifications [36–40,42] and the maintenance practices for the refrigeration systems [41,42] that are valid for open and semi-hermetic units and all applicable fluids.

1. The compressor suction pressure cannot be less than 0.2 bar [41,42].
2. Compressor discharge pressure cannot exceed 30 bar [36–40].
3. Gas temperature at the compressor suction cannot be less than 240 K [37].
4. Gas temperature at the compressor discharge can not exceed 393 K [36,41,42].

It is recommended that the compressor suction pressure be maintained above 1 bar. Nevertheless, it is allowed to lower it below this value [41,42]. This results in the possibility of air penetration into the system or overheating of the compressor motor in the case of semi-hermetic units. Figure 5 presents the modeling flowchart. The modeling started with the selection of fluids and parameters and variables: pressure drops in system components, heat rejection temperature T_M, compressor efficiency (see Table 2), and stage temperature difference (see Table 4).

Table 4. The modeling variables.

Name	Symbol	Unit	Value	References
Recuperation temperature difference	ΔT_{rec}	K	up to 73	[36,38]
Suction pressure	p_{suc}	bar	0.2–19 bar	[41,42]
Discharge pressure	p_{dis}	bar	p_{suc}—30 bar	[36–40]

Then, the first stage was designed as long as its operation is within assumed operational limits. This was done by adjusting the evaporation temperature and the mass flow. For stages with two-stage compression, an additional parameter is available, which is the pressure ratio of the second compressor π_{comp2}. After reaching the limits, the second stage and then the third stage were designed. If, because of the fluid selection, it was not possible to design the stage to reach proper temperatures, the modeling was interrupted. In this

way, certain fluids (R161, R218, R22, R32, R41) were eliminated from further analysis at the modeling stage.

The performance of the three-stage cascaded refrigeration system was expressed by means of the COP and Carnot efficiency, which refers the obtained COP compared to the Carnot COP. The Carnot efficiency allows one to eliminate the influence of the cooling power temperature T_0 on COP and to compare cases characterized by different cooling power temperatures. The COP of the system is expressed as the cooling power available in the third stage evaporator divided by the sum of the compressors' power demand:

$$COP = \frac{\dot{Q}_0}{\dot{N}_{comp,1} + \dot{N}_{comp,2} + \dot{N}_{comp,3}} \tag{18}$$

Carnot COP is obtained using heat rejection and cooling power temperatures:

$$COP_{Carnot} = \frac{T_0}{T_M - T_0} \tag{19}$$

Carnot efficiency is a ratio of COP and Carnot COP:

$$\eta_{Carnot} = \frac{COP}{COP_{Carnot}} \tag{20}$$

3. Results

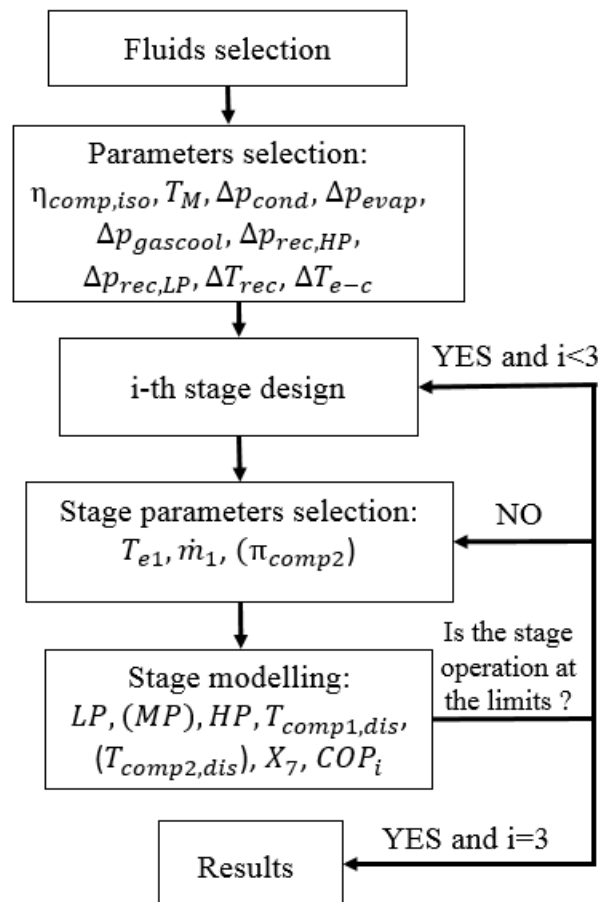The simulations performed are listed in Table 5 and presented in Figure 6.

Figure 6. Modeling flowchart.

Table 5. Considered refrigerant sets with respect to the normal boiling temperature range.

	1st Stage	2nd Stage	3rd Stage	COP	η_{Carnot}	T_0	FC
1.1	R125	R23	R14	0.229	0.257	147.4	A1
1.2	R290	R170	R14	0.268	0.302	147.1	A1 + A3
1.3	R1270	R1150	R14	0.284	0.312	149.2	A1 + A3
1.4	R125	R116	R14	0.187	0.216	145.1	A1
2.1	R290	R1150	R50	0.204	0.290	129.2	A3
2.2	R290	R170	R50	0.197	0.279	129.6	A3
2.3	R125	R1150	R50	0.179	0.262	127	A1 + A3
2.4	R125	R23	R14	0.184	0.240	135.8	A1
2.5	R125	R170	R50	0.168	0.242	128.3	A1 + A3

One can see that the application of single-stage compression in a three-stage cascaded system does not allow for the use of R50. This is not possible because to apply to R50 the evaporation temperature of around 172 K (saturation temperature at maximum discharge pressure) would have to have been achieved by means of two stages. The lack of the possibility to use R50 has a considerable impact on the cooling power temperatures reached, which for single-stage compression cases are not lower than 144 K. This was due to much higher evaporation temperatures with R14 than R50, which is clearly shown in Table 1. Moreover, a significant impact of flammable refrigerants can be seen in the enhancements in COP and Carnot efficiency. The sets of flammable fluids applied in simulations 1.2 and 1.3 resulted in 12–30% higher Carnot efficiency than those based only on non-flammable refrigerants (1.1, 1.4–1.6). This occurred due to the considerably greater heat of evaporation of flammable compounds. The application of two-stage compression significantly enhances the reachable cooling power temperatures: the discharge temperature limitation can be overcome (limitation of discharge pressure is still valid). This meant for R50 a cooling power temperature drop all the way down to 127 K. For two-stage compression systems with R14, the cooling power temperature did not drop below 135 K. The results show the general advantage of flammable refrigerants. The application of R290, R170, R1150, R1270 or R50 allows for a significant increase in Carnot efficiency compared to other refrigerants. This results from considerably greater heat of evaporation of flammable compounds, which can be seen in Table 1.

One of the most substantial operational limits of refrigeration compressors is the gas discharge temperature, which cannot exceed 393 K. This puts a significant limitation on the pressure ratio obtained, which, in turn, affects the stage temperature difference (the difference between the condensation and evaporation temperatures of the stage). The gas discharge temperature can be lowered by lowering the gas suction temperature. In the case of the analyzed system, this can be achieved by increasing the recuperation temperature difference ΔT_{rec} or by two-stage compression. An increased recuperation temperature difference can keep the gas discharge temperature within the limits, but at the expense of a reduced COP because of worsened recuperation. Figures 7–9 present the influences of the difference in recuperation temperature on the applicability and performances of three different refrigerant kits: flammable (R290, R1150, R50), non-flammable (R125, R23, R14) and mixed (R125, R1150, R50). Due to the limitation of the suction gas temperature to at least 240 K, the recuperation temperature difference cannot be greater than 73 K. The results show that the application of flammable and mixed sets of refrigerants (flammable along with non-flammable) requires a recuperation temperature difference of at least 55 K for mixed refrigerants and 61 K for flammable. For a non-flammable refrigerant kit, the recuperation temperature difference can be much lower. Increasing the recuperation temperature difference is crucial for the applicability of the given refrigerant kits and reachable cooling power temperatures. This is done at the expense of systems' COP, and it causes, despite a cooling power temperature drop, a decrease in Carnot efficiency.
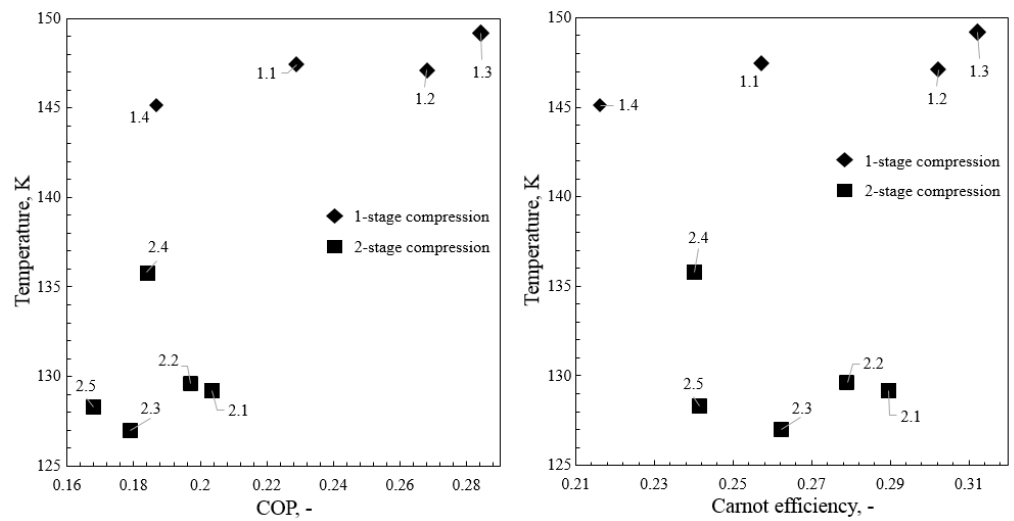
Figure 7. The performances of the analyzed refrigerant configurations.
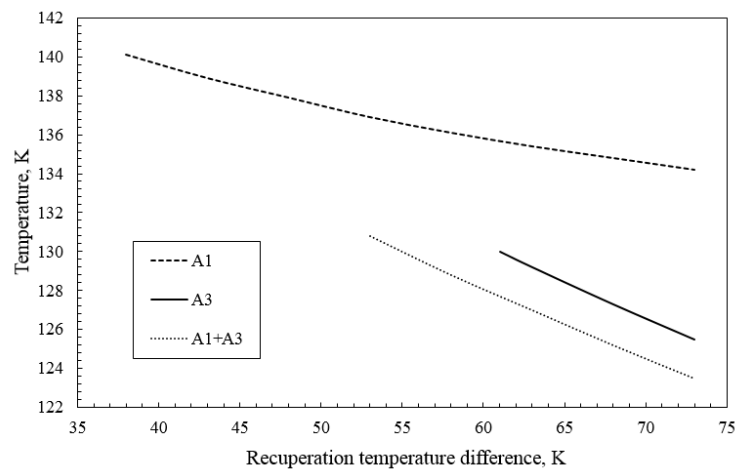

Figure 8. The cooling power temperatures of flammable (A3: R290, R1150, R50), non-flammable (A1: R125, R23, R14) and mixed (A1 + A3:R125, R1150, R50) refrigerant configurations with respect to recuperation temperature difference.
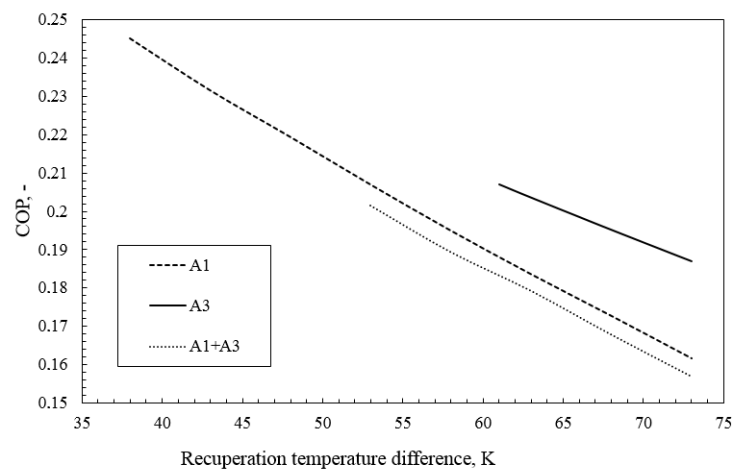

Figure 9. The COP of flammable (A3: R290, R1150, R50), non-flammable (A1: R125, R23, R14) and mixed (A1 + A3:R125, R1150, R50) refrigerant configurations with respect to the difference in recuperation temperature.

The performance of the complete system depends on the performance of each stage; therefore, Figures 10–12 present the performances of the first, second and third stages, respectively. Stage performance is expressed as stage temperature difference (the difference between stage condensation and evaporation temperatures), COP and Carnot efficiency. In Figure 10, one can see that the first stage has the highest potential for decreasing temperature. The temperature differences range from 88 to 103 K, which means that within the given limitations, the evaporation temperature of 210 K can be reached. Such a great temperature difference results in a reduction in COP ranging from 0.6 to 1.1, which corresponds to 0.3 to 0.42 Carnot efficiency. This also confirms that two-stage compression in cases of the first system stage not being required. It is due to the fact that refrigerants matching the first stage have complex molecules which are characterized by lower heat capacity ratios. This significantly affects the discharge temperature.
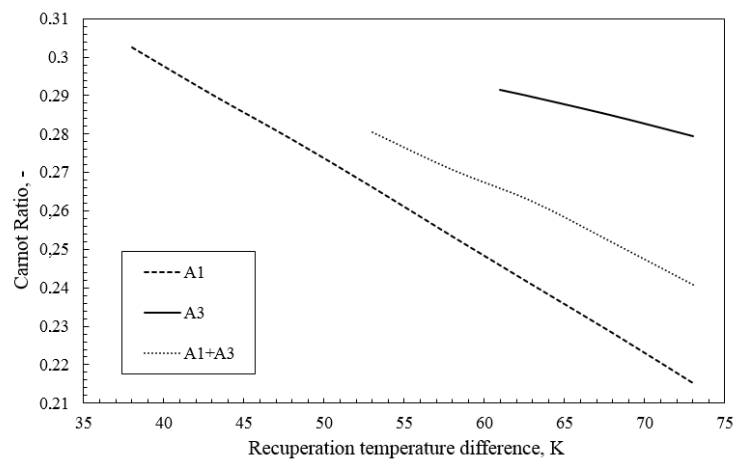

Figure 10. The limiting Carnot efficiency of flammable (A3: R290, R1150, R50), nonflammable (A1: R125, R23, R14) and mixed (A1+A3: R125, R1150, R50) refrigerant configurations with respect to recuperation temperature difference.
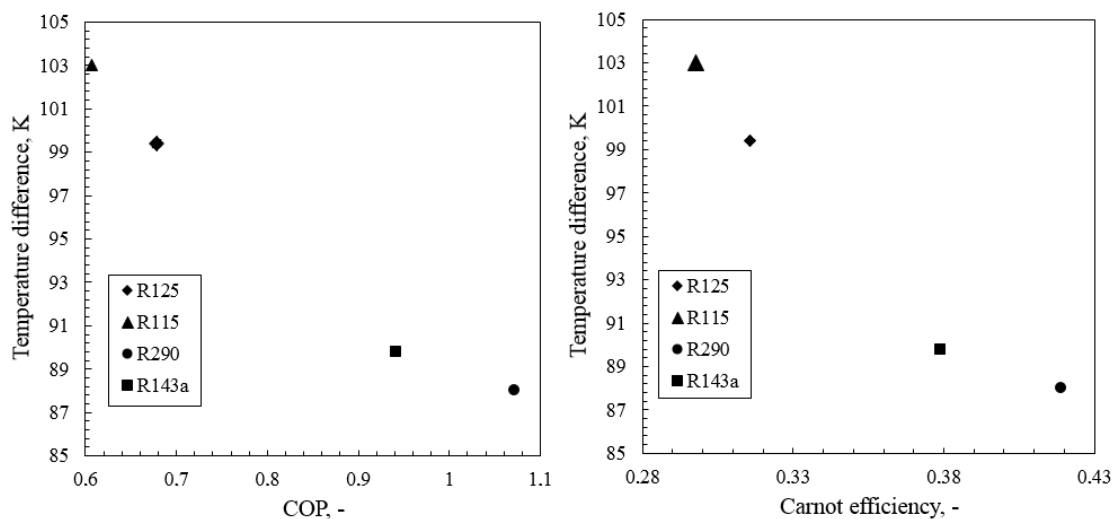

Figure 11. The performances of first stage refrigerants.

Figure 11 presents the performance of the second stage with respect not only to the applied refrigerant but also to the type of compression (single stage or two stage). Application of two-stage compression allows one to enhance the stage temperature difference. The highest temperature differences can be obtained using R13 (non-zero-ODP refrigerant) and flammable refrigerants R170 and R1150. The application of zero-ODP refrigerants from the A1 group limits the temperature difference to less than 35 K.
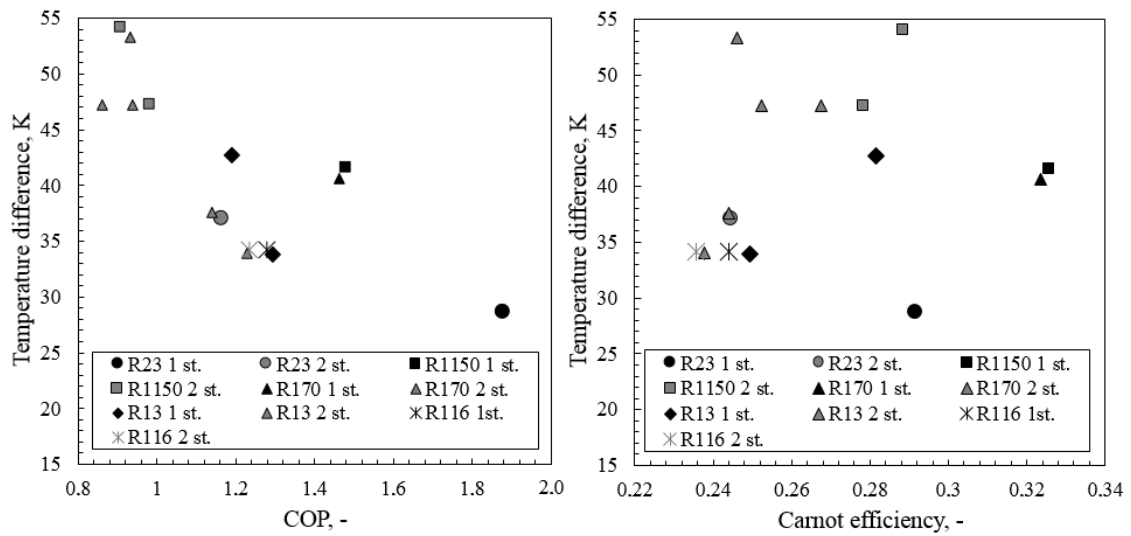
Figure 12. The performance of second-stage refrigerants.

Figure 12 presents the performance of the third stage of the three-stage cascaded refrigeration system. This stage can be realized only by applying R14 or R50 (only by using two-stage stage compression). The temperature difference was limited to 40 K for single-stage compression and 43 K for two-stage compression. Such a small increase in the temperature difference for two-stage compression resulted from a lower covered temperature range: R50 can be applied only if the condensation temperature of about 172 K is satisfied (due to the compressor pressure limitation). In contrast, R14 requires only a condensation temperature of 220 K.

A factor which also limits the applicability of three-stage cascaded refrigeration systems is the gas suction pressure of the compressors. Lowering the gas suction pressure reduces the evaporation temperature, but on the other hand, the decrease leads to an increase in required volumetric capacity of the compressor, and increases in the pressure ratio and in gas discharge temperatures—or, in the case of semi-hermetic compressors, to technical problems, such as overheating of the electric motor winding. Operation of the system with subatmospheric pressures will also reverse the consequences of leakage: instead of rejecting the refrigerant into the atmosphere, air will be sucked into the system, causing its contamination. Figures 13 and 14 show the gas suction pressures for each stage for each of the cases analyzed.
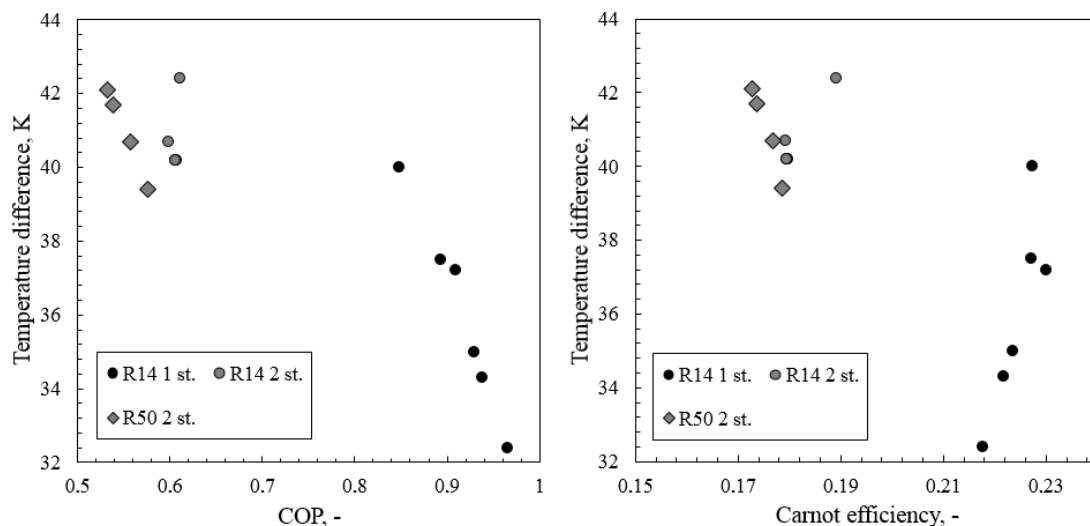

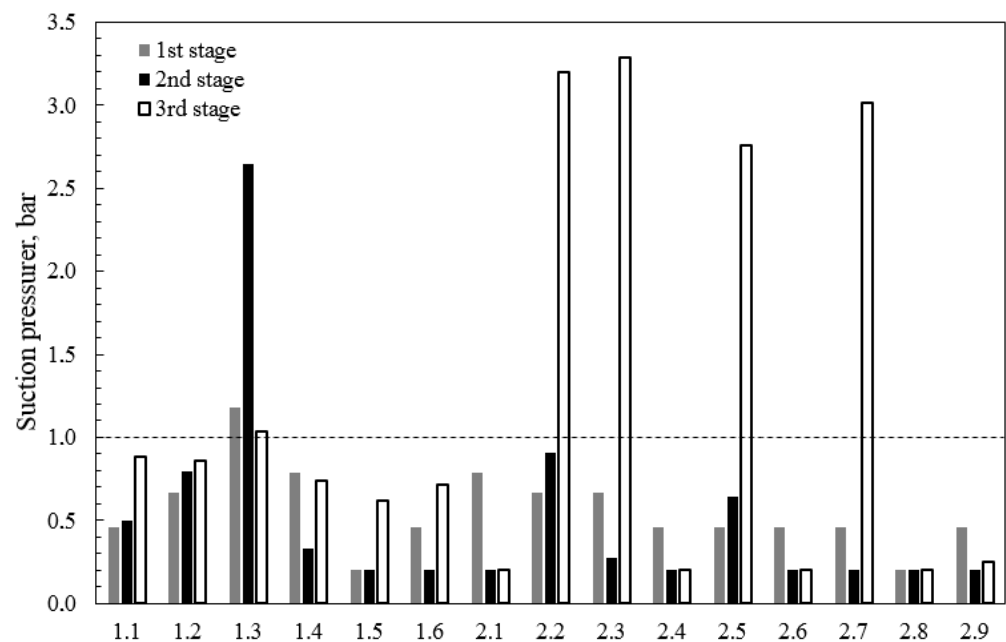**Figure 13.** The performance of third-stage refrigerants.

Figure 14. Suction pressures of the compressors during suction for the analyzed refrigeran configurations.

It can be seen that most of the cases analyzed require operation with subatmospheric gas suction pressures. Only case 1.3 operates with all gas suction pressures above 1 bar, but this, according to Figure 5, results in a cooling power temperature of around 150 K. This significantly limits the applications of such systems: LNG could be reliquefied only under saturation pressures greater than 10 bar. Furthermore, the refrigerant configuration is based on flammable R1270 and R1150, which are not allowed in many cryogenic applications, such as cryotherapy. To mitigate the issue of a low suction pressure, the following approaches can be used:

1. Limit the cooling power temperature to the saturation temperature corresponding to 1 bar. This approach is applicable only to R14 and would limit the cooling power temperature to 144.9 K.
2. Minimization of pressure drops. The assumed evaporator and recuperator pressure drops comprise 10% of the gas suction pressure. Therefore, minimizing these losses can increase the gas suction pressure by 20%.
3. Increasing number of stages. Ultimately, the number of stages would probably need to increase to four. This significantly increases the complexity of the system and questions the legitimacy of the use of such systems.

4. Conclusions

The potential utilization of a three-stage cascaded refrigeration system based on standard refrigeration equipment for cryogenic applications was assessed. A group of refrigerants—flammable, non-flammable and zero-ODP—were considered. Cascaded refrigeration system modeling was performed, providing vital information on the overall system and particular stages' performances and refrigerant configuration limitations. Theoretical analysis led to the following conclusions:

1. A three-stage cascaded refrigeration system based on standard mass-produced refrigeration equipment can provide cooling power at a temperature of 130 K with COP greater than 0.17.
2. The application of flammable refrigerants substantially improves the performance of the cryorefrigerator. The use of only non-flammable refrigerants is possible, but it puts significant limitations on the cooling power temperature and COP of the system.

3. The use of two-stage compression at the second and third stages allows one to improve the performance. Furthermore, due to two-stage compression, it is possible to apply R50 as a third-stage refrigerant which requires the evaporating temperature in the second stage to be as low as 186 K.
4. The recuperation temperature difference is a vital parameter for the feasibility of systems analyzed using flammable refrigerants. It allows one to meet the strict requirements of refrigeration compressors.
5. To reach a cooling power temperature of 130 to 150 K, the three-stage cascaded refrigerator usually operates with lower gas suction pressures than atmospheric. The requirement of operation at suction pressures of at least 1 bar will significantly reduce the feasibility and performance of the analyzed systems.

Abbreviations

The following abbreviations are used in this manuscript:

Symbol	Description	Unit
Latin		
$\dot{N}$	Power	W
Q	Quality	-
p	Pressure	bar
s	Specific entropy	J kg^{-1} K^{-1}
T	Temperature	K
Greek		
ΔH_{ev}	Heat of evaporation	kJ kg^{-1}
Δp	Pressure drop	bar
ΔT	Temperature difference	K
η	Efficiency	-
Abbreviations		
COND	Condenser	
COP	Coefficient of Performance	
EVAP	Evaporator	
GAS COOL	Gas Cooler	
GWP	Global Warming Potential	
LNG	Liquified Natural Gas	
NG	Natural Gas	
ODP	Ozone depletion Potential	
REC	Recuperation	
Subscripts		
0	refers to cooling power	
Carnot	refers to Carnot cycle	
comp	compressor	
cond	condenser	

cr	critical point
ev	evaporator
e-c	evaporator-condenser
gascool	gas cooler
HP	high pressure
LP	low pressure
M	refers to heat sink
rec	recuperation
s	isentropic
TP	triple point
sat	saturated

References

1. Rogala, Z.; Brenk, A.; Malecha, Z. Theoretical and Numerical Analysis of Freezing Risk During LNG Evaporation Process. *Energies* **2019**, *12*, 1426. [CrossRef]
2. Barclay, M.; Gangaware, D.F.; Dalton, K.; Skrzypkowski, M. Thermodynamic Cycle Selection for Distributed Natural Gas Liquefaction. *Aip Conf. Proc.* **2016**, *75*, 710
3. Pauli, G. Refrigeration Loops in LNG Applications: Dynamic Simulation and Optimization Study. Ph.D. Thesis, Università di Pisa, Pisa, Italy, 2018.
4. Kamalinejad, M.; Amidpour, M.; Naeynian, S.M.M. Thermodynamic design of a cascade refrigeration system of liquefied natural gas by appling mixed integer non-linear programming. *Chin. J. Chem. Eng.* **2015**, *23*, 998–1008. [CrossRef]
5. Kamalinejad, M.; Amidpour, M.; Naenian, M.M. Optimal Synthesis of Cascade Refrigeration in Liquefied Natural Gas Cycles by Pinch-Exergy. *J. Oil Gas Petrochem. Technol.* **2013**, *1*, 29–44.
6. Trigilio, A.; Bouza, A.; Scipio, S.D. Modelling and Simulation of Natural Gas Liquefaction Process. *J. Nat. Gas Sci. Eng.* **2016**, *28*, 672–690. Available online: https://www.intechopen.com/chapters/35292 (accessed on 13 June 2022).
7. Ghorbani, B.; Hamedi, M.H.; Amidpour, M. Cascade refrigeration systems in integrated cryogenic natural gas process (natural gas liquids (NGL), liquefied natural gas (LNG) and nitrogen rejection unit (NRU)). *Energy* **2016**, *115*, 88–106. [CrossRef]
8. Shariq, M.; Karimi, I.A.; Wood, D.A. Retrospective and future perspective of natural gas liquefaction and optimization technologies contributing to ef fi cient LNG supply: A review. *J. Nat. Gas Sci. Eng.* **2017**, *45*, 165–188.
9. Lin, W.; Xiong, X.; Gu, A. Optimization and thermodynamic analysis of a cascade PLNG (pressurized liquefied natural gas) process with CO_2 cryogenic removal. *Energy* **2018**, *161*, 870–877. [CrossRef]
10. Kochunni, S.K.; Chowdhury, K. Comparison between reverse Brayton and Kapitza based LNG boil-off gas reliquefaction system using exergy analysis Comparison between reverse Brayton and Kapitza based LNG boil-off gas reliquefaction system using exergy analysis. In Proceedings of the IOP Conference Series: Materials Science and Engineering, 26th International Cryogenic Engineering Conference & International Cryogenic Materials Conference 2016, New Delhi, India, 7–11 March 2016; IOP Publishing Ltd.: Bristol, UK, 2016.
11. Johnson, A.N.; Baltrusiatis, J.; William, L.; Johnson, N. Design and Control of a Cryogenic Multi-Stage Compression Refrigeration Process. *Chem. Eng. Res. Des.* **2017**, *121*, 360–367. [CrossRef]
12. Yousef, A.M.; Eldrainy, Y.A.; El-maghlany, W.M.; Attia, A. Biogas upgrading process via low-temperature CO_2 liquefaction and separation. *J. Nat. Gas Sci. Eng.* **2017**, *45*, 812–824. [CrossRef]
13. Baranov, A.Y.; Malysheva, T.A. Turbo-refrigerators using for cooling the cryotherapeutic units. *Procedia Eng.* **2016**, *152*, 169–172. [CrossRef]
14. Little, W.A.; Sapozhnikov, I. *Low Cost Cryocoolers for Cryoelectronics*; Springer: Berlin/Heidelberg, Germany, 1997; pp. 509–513.
15. Kainin, S.; Ponchunchoovong, S.; Imsilp, U.; Singsee, S. Cryopreservation of Mekong catfish , Pangasius bocourti Sauvage, spermatozoa. *Aquac. Res.* **2014**, *45*, 859–867. [CrossRef]
16. Choi, M.J.; Abduzukhurov, T.; Park, D.H.; Kim, E.J. Effects of Deep Freezing Temperature for Long-term Storage on Quality Characteristics and Freshness of Lamb Meat. *Korean J. Food Sci. Anim. Resour.* **2018**, *38*, 959–969. [CrossRef]
17. Kumar, N.; Biswas, K. Cryomilling: An environment friendly approach of preparation large quantity ultra refined pure aluminium nanoparticles. *J. Mater. Res. Technol.* **2019**, *8*, 63–74. [CrossRef]
18. Hou, Q.; Shi, Z.C.; Fan, R.H.; Ju, L.C. Cryomilling and Characterization of Metal/ceramic Powders. *Key Eng. Mater.* **2012**, *512–515*, 127–131. [CrossRef]
19. Enayati, M.H. Nanocrystallization of Al Powder by Cryomilling Process. *KONA Powder Part. J.* **2017**, *34*, 207–212. [CrossRef]
20. Zhou, F.; Witkin, D.; Nutt, S.R.; Lavernia, E.J. Formation of nanostructure in Al produced by a low-energy ball milling at cryogenic temperature. *Mater. Sci. Eng. A* **2004**, *375–377*, 917–921. [CrossRef]
21. Romero-gomez, J.; Romero-gomez, M.; Ferreiro Garcia, R.; De Miguel Catoira, A. On board LNG reliquefaction technology: A comparative study. *Pol. Marit. Res.* **2014**, *21*, 77–88. [CrossRef]

22. Xiong, L.; Peng, N. Optimization of UA of heat exchangers and BOG compressor exit pressure of LNG boil-off gas reliquefaction system using exergy analysis. In Proceedings of the IOP Conference Series: Materials Science and Engineering, Advances in Cryogenic Engineering: Proceedings of the Cryogenic Engineering Conference (CEC) 2015, Tucson, AZ, USA, 28 June–2 July 2015; IOP Publishing Ltd.: Bristol, UK, 2015.

23. Sayyaadi, H.; Babaelahi, M. Exergetic Optimization of a Refrigeration Cycle for Re-Liquefaction of LNG Boil-Off Gas. *Int. J. Thermodyn.* **2010**, *13*, 127–133.

24. Quack, H. Theory of cascade refrigeration. *Aip Conf. Proc.* **2012**, *783*, 1434.

25. Kanizawa, F.T.; Ribatski, G. Modeling and analysis of a cascade cryogenic refrigerator. In Proceedings of the 22nd International Congress of Mechanical Engineering, Ribeirã o Preto, SP, Brazil, 3–7 November 2013.

26. Lee, S.; Choi, S.H.; Lee, Y.; Cha, K.; Young-myung, Y. The study on a new liquefaction cycle development for LNG plant. In Proceedings of the International Gas Union Research Conference, Seoul, Korea, 19–21 October 2011.

27. Dorosz, P.; Chorowski, M.; Piotrowska, A. Performance of the one-stage Joule–Thomson cryocooler fed with a nitrogen–hydrocarbon mixture and built from mass-produced components made for the refrigeration industry. *Int. J. Refrig.* **2017**, *82*, 252–261. [CrossRef]

28. Dorosz, P.; Piotrowska, A.; Pyrka, P.; Bogdan, P. Analysis of the LNG re-condensation system based on Joule-Thomson cooler. In Proceedings of the IOP Conference Series: Materials Science and Engineering, 27th International Cryogenics Engineering Conference and International Cryogenic Materials Conference 2018 (ICEC-ICMC 2018), Oxford, UK, 3–7 September 2018; IOP Publishing Ltd.: Bristol, UK, 2019.

29. Piotrowska, A.; Chorowski, M.; Dorosz, P. Performance Analysis of Joule-Thomson Cooler Supplied with Gas Mixtures. In Proceedings of the IOP Conference Series: Materials Science and Engineering, 26th International Cryogenic Engineering Conference & International Cryogenic Materials Conference 2016, New Delhi, India, 7–11 March 2016; IOP Publishing Ltd.: Bristol, UK, 2017.

30. Missimer, D. Refrigerant conversion of Auto-Refrigerating Cascade (ARC) systems. *Int. J. Refrig.* **1997**, *20*, 201–207. [CrossRef]

31. Lee, C.; Yoo, J.; Jin, L.; Cha, J.; Jeong, S. Development of Cascade Non- F lammable Mixed Refrigerant Joule-Thomson Refrigerator for 100 K. In Proceedings of the 19th International Cryocooler Conference (ICC19), San Diego, CA, USA, 20–23 June 2016; pp. 385–394.

32. Chakravarthy, V.; Wber, J.; Rashad, A.A.; Acharya, A.; Bonaquist, D. Oxygen liquefier using a mixed gas refrigeration cycle. In Proceedings of the ASME International Mechanical Engineering Congress, Washington, DC, USA, 15–21 November 2003.

33. Lee, H.S.; Oh, S.T.; Yoon, J.I.; Lee, S.G.; Choi, K.H. Analysis of Cryogenic Refrigeration Cycle using Two Stage Intercooler. *Defect Diffus. Forum* **2010**, *297–301*, 1146–1151. [CrossRef]

34. Qyyum, M.A.; Ali, W.; Long, N.V.D.; Khan, M.S.; Lee, M. Energy efficiency enhancement of a single mixed refrigerant LNG process using a novel hydraulic turbine. *Energy* **2017**, *144*, 968–976. [CrossRef]

35. European Union. *Regulation (EU) No 517/2014 of the Council on Fluorinated Greenhouse Gases and Repealing Regulation*; Technical Report; European Union: Brussels, Belgium, 2014.

36. Bock Kaltemaschinen. Operating Instructions Semi-Hermetic Motorcompressors. Technical Report 09963. Available online: https://www.gea.com/pl/productgroups/compressors/compressors-for-commercial-refrigeration/semi-hermetic-compressors/index.jsp (accessed on 12 May 2020).

37. GEA-Bock. *Semi-Hermetic GEA Bock Compressors*; Technical Report; GEA-Bock: Frickenhausen, Germany, 2020

38. Frascold. *Frascold Data Sheets Q4-21.1Y*; Technical Report; Frascold: Rescaldina, Italy, 2020

39. Frascold. *Frascold Data Sheets CXH01-80-298Y*; Technical Report; Frascold: Rescaldina, Italy, 2020

40. Bitzer. *Bitzer Semi-Hermetic Reciprocating Compressors Technical Data 4FES-5Y*; Technical Report; Bitzer: Sindelfingen, Germany, 2020

41. Hundy, G.F.; Trott, A.R.; Welch, T.C. *Refrigeration, Air Conditioning and Heat Pumps*, 5th ed.; Butterworth-Heinemann: Oxford, UK, 2016.

42. *Refrigeration Manual Part 4—System Design*; Technical Report; Emerson: St. Louis, MI, USA, 1969.

43. Lemmon, E.W.; Bell, I.H.; Huber, M.L.; McLinden, M.O. *NIST Standard Reference Database 23: Reference Fluid Thermodynamic and Transport Properties-REFPROP*; Version 10.0; National Institute of Standards and Technology: Gaithersburg, MD, USA, 2018.

44. Bell, I.H.; Wronski, J.; Quoilin, S.; Lemort, V. Pure and Pseudo-pure Fluid Thermophysical Property Evaluation and the Open-Source Thermophysical Property Library CoolProp. *Ind. Eng. Chem. Res.* **2014**, *53*, 2498–2508. [CrossRef]

45. Frascold Semihermetic Compressors. Available online: https://www.frascold.it/en/products/technologies/reciprocating_compressors (accessed on 12 May 2020).

46. Dorin Semihermetic Compressors. Available online: https://www.dorin.com/en/catalogo-15/SE/ (accessed on 12 May 2020).

47. Wang, H.; Chen, G.; M.Q., G.; Li, X. Performance comparison of single-stage mixed- refrigerant Joule–Thomson cycle and reverse Brayton cycle for cooling 80 to 120 K temperature- distributed heat loads. In Proceedings of the IOP Conference Series: Materials Science and Engineering, Advances in Cryogenic Engineering: Proceedings of the Cryogenic Engineering Conference (CEC) 2017 (Previous Edition: CEC-2015), Madison, WI, USA, 9–13 July 2017; IOP Publishing Ltd.: Bristol, UK, 2017. [CrossRef]

48. Lee, C.; Jin, L.; Park, C.; Jeong, S. Design of non-flammable mixed refrigerant Joule-Thomson refrigerator for precooling stage of high temperature superconducting power cable Design of non-flammable mixed refrigerant Joule-Thomson refrigerator for precooling stage of high temperature superco. *Cryogenics* **2017**, *81*, 14–23. [CrossRef]

49. Kruthiventi, S.A.I.S.; Govindharasu, N.; Rao, Y.V.H. An identification of best mixture composition for the Joule-Thomson refrigerator operating at 90 K. *Int. J. Mech. Prod. Eng. Res. Dev.* **2018**, *8*, 467–476.

50. Kochenburger, T.M.; Oellrich, L.R. Evaluation of a two-stage mixed refrigerant cascade for HTS cooling below 60 K. *Phys. Procedia* **2015**, *67*, 227–232. [CrossRef]

51. Jensen, J.B.; Skogestad, S. Optimal Operation of a Simple Lng Process. *IFAC Proc. Vol.* **2006**, *39*, 241–246. [CrossRef]

52. Lee, J.; Oh, H.; Jeong, S. Investigation of neon—nitrogen mixed refrigerant Joule—Thomson cryocooler operating below 70 K with precooling at 100 K. *Cryogenics* **2014**, *61*, 55–62. [CrossRef]

53. Chang, H.m. A thermodynamic review of cryogenic refrigeration cycles for liquefaction of natural gas. *Cryogenics* **2015**, *72*, 127–147. [CrossRef]